

Theory of orientational epitaxy in the self-consistent phonon approximation

Anthony D. Novaco

Lafayette College, Easton, Pennsylvania 18042

and Brookhaven National Laboratory, Upton, New York 11973

(Received 8 March 1978; revised manuscript received 18 December 1978)

The theory of the orientational epitaxy phase is developed for an anharmonic solid monolayer within the framework of a self-consistent phonon approximation. This theory shows how the adatom-adatom coupling constants and adatom-substrate coupling constants in the theory of Novaco and McTague are modified by renormalization due to the zero-point motion and the thermal vibration of the adatoms. Some general conclusions about the nature of orientational epitaxy are presented and numerical results are given for argon adsorbed on basal plane graphite. These results show that while many calculated properties of the argon solid have important corrections due to the anharmonic nature of the system, the orientation angle versus lattice constant curve is not affected to any significant degree.

I. INTRODUCTION

The structure of a solid monolayer (or single layer "crystal") in the field of a solid substrate surface is an important problem which has received much attention over many years.¹⁻⁴ The interest in this problem is due, in part, to the general interest in the study of gases adsorbed on solid surfaces.^{5,6} The study of the monolayer problem is also relevant to the study of the interface between two crystalline solids¹ and to the study of how dimensionality affects phase transitions.⁵ Generally, the monolayer and the substrate lattices are incommensurate, that is, they have no common unit cell. The response of each lattice to the perturbing field of the other generates a structure within each lattice which is incommensurate with both parent lattices. The physics of these coupled lattices has, naturally, much in common with other incommensurate structures such as charge-density waves in metals and spin-density waves in magnetic materials.^{7,8}

Recent theoretical and experimental work on the adsorption of rare-gas monolayers on graphite has demonstrated the existence of a new phase which exhibits a rather striking phenomenon called orientational epitaxy.⁹⁻¹¹ This effect is the rotational locking of the monolayer to the substrate surface even when these lattices are incommensurate. It is generated by the existence of static mass-density waves (MDWs) in the monolayer, these MDWs being "frozen" displacement waves caused by the external periodic field of the substrate. Assuming this field is incommensurate with the monolayer lattice, the angle at which the two lattices are locked is generally a nonsymmetry angle because it depends upon the lattice dynamics of the monolayer as well as the degree of

misfit between the two lattices. The recently published theory of orientational epitaxy used both the linear response and harmonic approximations to investigate the physics of this new phase.⁹ It is shown here how these limitations can be removed while still retaining the picture of noninteracting phonons. After discussing the general approach, the equations which describe the "large" oscillation and "small" distortion limit are derived as a special case. The relation of the large distortion limit to the generation of higher harmonic distortions and mixed phonon states is discussed briefly. The general approach is to search for the "best" phonon representation for a monolayer interacting with a fixed substrate. Even in the large distortion limit, this procedure would be a logical first step in the construction of a general theory. The present theory is then a self-consistent phonon¹² calculation (SCP) now with both the adatom-adatom coupling constants and the adatom-substrate coupling constants renormalized by the oscillations of the atoms about their equilibrium positions. Within the small distortion limit, the results quoted here are formally the same as the earlier work of Novaco and McTague⁹ except here all coupling constants are renormalized.

A commonly used model for the monolayer is the two-dimensional approximation where the atoms are restricted to a plane and the substrate is replaced by an external field which acts in this space. This model has most of the important physics of the actual problem⁹ and so we use it here. The general theory is developed at finite temperatures and without any restriction in the dimensionality of the system. How the two-dimensional nature of the monolayer model and finite temperature aspects of the calculation are to be reconciled with Mermin's theorem¹³ on the ab-

sence of crystalline long-range order in two dimensions will be discussed after the results are presented.

The numerical results for argon adsorbed on graphite show important anharmonic corrections to the lattice dynamics of the argon solid due to the zero-point motion of the atoms. There are corresponding changes in both the intramonolayer and monolayer-substrate energy terms. The SCP values for the amplitudes of the strains are about 30% smaller than the quasiharmonic (QH) values, but the orientation angle at fixed lattice constant differs by less than 5% from its QH value. This small change in the orientation angle is due to the small shift in the ratio of transverse to longitudinal sound velocities produced by the SCP corrections. The orientation angle has been measured for argon on graphite, and the calculated values agree very well with the experimental ones.¹¹

II. SELF-CONSISTENT PHONON THEORY

The Hamiltonian of the monolayer in the presence of a static, periodic substrate potential field is taken to be

$$\hat{H} = \hat{K} + \hat{\Phi} + \hat{U}, \quad (1)$$

where \hat{K} is the kinetic energy, $\hat{\Phi}$ is the two-body adatom-adatom potential energy, and \hat{U} is the one-body adatom-substrate potential energy. If R_j^α represents the α component of the ideal (undistorted) lattice site of the j th adatom, \hat{u}_j^α represents the α component of the displacement of this particle from its ideal site, and \hat{p}_j^α represents the α component of its momentum; then using the Einstein convention for summations over components

$$\hat{K} = \frac{1}{2M} \sum_j \hat{p}_j^\alpha \hat{p}_j^\alpha, \quad (2a)$$

$$\hat{\Phi} = \frac{1}{2} \sum_{ij} \gamma_{ij} \sum_{\vec{q}} \tilde{V}_q e^{i\vec{q} \cdot (\vec{R}_i - \vec{R}_j)} e^{iq^\alpha (\hat{u}_i^\alpha - \hat{u}_j^\alpha)}, \quad (2b)$$

$$\hat{U} = \sum_j \sum_{\vec{G}} U_{\vec{G}} e^{i\vec{G} \cdot \vec{R}_j} e^{iG^\alpha \hat{u}_j^\alpha}, \quad (2c)$$

where M is the mass of the adatom, V_q is the Fourier transform of the two-body potential, and $U_{\vec{G}}$ is the Fourier coefficient of the one-body potential associated with the (substrate lattice) reciprocal lattice vector \vec{G} . The quantity γ_{ij} is equal to one for $i \neq j$ and equal to zero for $i = j$. The symbol $\sum_{\vec{q}}$ represents the sum over all values of \vec{q} in the two-dimensional space. This is to be distinguished from $\sum_{\vec{q}}$ (no tilde) which will represent the sum over all \vec{q} in the first Brillouin zone of the undistorted solid.

The usual creation and destruction operators $\hat{a}_{\vec{p},l}^\dagger$ and $\hat{a}_{\vec{p},l}$ for phonons with momentum \vec{p} and polariza-

tion l are introduced via the transformation

$$\hat{u}_j^\alpha = \frac{1}{N^{1/2}} \sum_{\vec{q},l} \epsilon_l^\alpha(\vec{q}) \exp(i\vec{q} \cdot \vec{R}_j) \times \left(\frac{\hbar}{2M\omega_l(\vec{q})} \right)^{1/2} (\hat{a}_{\vec{q},l} + \hat{a}_{-\vec{q},l}^\dagger), \quad (3a)$$

$$\hat{p}_j^\alpha = \frac{i}{N^{1/2}} \sum_{\vec{q},l} \epsilon_l^\alpha(\vec{q}) \exp(-i\vec{q} \cdot \vec{R}_j) \times \left(\frac{M\hbar\omega_l(\vec{q})}{2} \right)^{1/2} (\hat{a}_{\vec{q},l}^\dagger - \hat{a}_{-\vec{q},l}). \quad (3b)$$

The polarization vectors $\epsilon_l^\alpha(\vec{q})$ and the frequencies $\omega_l(\vec{q})$ are to be considered variational parameters which are determined by minimizing an approximate form of the Helmholtz free energy F subject to the $\epsilon_l^\alpha(\vec{q})$ satisfying the usual orthonormal constants. If the $\langle \hat{H} \rangle$, where $\langle \dots \rangle$ is the ensemble average, were calculated by taking the diagonal part of \hat{H} in the above phonon basis set and this were used in the calculation of F , then the standard equations for self-consistent phonon theory would be reproduced upon the minimization of F .¹⁴ However, such a procedure guarantees that $\langle \hat{u}_j^\alpha \rangle = 0$, and this condition is inconsistent with $\hat{U} \neq 0$. A nonzero value of $\langle \hat{u}_j^\alpha \rangle$ implies a nonzero value of both $\langle \hat{a}_{\vec{p},l}^\dagger \rangle$ and $\langle \hat{a}_{-\vec{p},l} \rangle$. This effect can be incorporated into a new set of phonon modes through the displaced oscillator transformation on the $\hat{a}_{\vec{p},l}^\dagger$ and $\hat{a}_{-\vec{p},l}$ operators. This canonical transformation to new phonon operators $\hat{\alpha}_{\vec{p},l}^\dagger$ and $\hat{\alpha}_{-\vec{p},l}$ is given by the equations

$$\hat{a}_{\vec{p},l}^\dagger = N^{1/2} \zeta_{\vec{p},l}^* \hat{\alpha}_{\vec{p},l}^\dagger + \hat{\alpha}_{\vec{p},l}^\dagger, \quad (4a)$$

and

$$\hat{a}_{-\vec{p},l} = N^{1/2} \zeta_{\vec{p},l} \hat{\alpha}_{-\vec{p},l} + \hat{\alpha}_{-\vec{p},l}, \quad (4b)$$

where $\zeta_{\vec{p},l}$ and $\zeta_{\vec{p},l}^*$ are c numbers determined by the conditions

$$\langle \hat{\alpha}_{\vec{p},l}^\dagger \rangle = \langle \hat{\alpha}_{-\vec{p},l} \rangle = 0$$

and by the minimization of the free energy. The new phonon operators $\hat{\alpha}_{\vec{p},l}^\dagger$ and $\hat{\alpha}_{-\vec{p},l}$ describe the oscillation of each adatom about its statically displaced equilibrium point $R_j^\alpha + \langle \hat{u}_j^\alpha \rangle$. These new operators are related to $\delta \hat{u}_j^\alpha = \hat{u}_j^\alpha - \langle \hat{u}_j^\alpha \rangle$ by the same transformation which relates the old phonon operators to \hat{u}_j^α . The $\langle \hat{H} \rangle$ is now calculated by taking the diagonal elements in the α -basis set. These new phonon states are then treated as a set of noninteracting modes with S , the entropy, being the standard boson functional of

$$n_l(\vec{p}) = \langle \hat{\alpha}_{\vec{p},l}^\dagger \hat{\alpha}_{\vec{p},l} \rangle,$$

(see Ref. 15) the average occupation number of the

(\bar{p}, l) mode. The free energy $F = \langle \hat{H} \rangle - TS$ is now a functional of the quantities

$$\epsilon_l^\alpha(\bar{p}), \omega_l(\bar{p}), \zeta_{\bar{p}, l}^*, \zeta_{\bar{p}, l}$$

and $n_l(\bar{p})$. In calculating $\langle \hat{H} \rangle$, the well-known property of the harmonic oscillator wave functions is used to replace the average of the exponential by the exponential of averages.¹⁶

The variational calculation is carried out in a straightforward although somewhat tedious fashion. We begin by defining order parameters $u_{\bar{q}}^\alpha$ and $v_{\bar{q}}^\alpha$ for the new phase. These order parameters are given by

$$u_{\bar{q}}^\alpha = \sum_l \epsilon_l^\alpha(\bar{q}) \left(\frac{\hbar}{2M\omega_l(\bar{q})} \right)^{1/2} (\zeta_{\bar{q}, l} + \zeta_{-\bar{q}, l}^*), \quad (5a)$$

$$v_{\bar{q}}^\alpha = i \sum_l \epsilon_l^\alpha(\bar{q}) \left(\frac{M\hbar\omega_l(\bar{q})}{2} \right)^{1/2} (\zeta_{\bar{q}, l}^* - \zeta_{-\bar{q}, l}). \quad (5b)$$

The $u_{\bar{q}}^\alpha$ and $v_{\bar{q}}^\alpha$ are just the Fourier amplitudes associated with $\langle \hat{u}_j^\alpha \rangle$ and $\langle \hat{p}_j^\alpha \rangle$ respectively, as can easily be seen by comparing Eqs. (5) to Eqs. (4) and Eqs. (3). It is convenient to carry out the variation of the free energy with respect to the $u_{\bar{q}}^\alpha$ and $v_{\bar{q}}^\alpha$ instead of the $\zeta_{\bar{q}, l}$ and $\zeta_{-\bar{q}, l}^*$. The $\langle \hat{K} \rangle$ is found to be given by

$$\begin{aligned} \langle \hat{K} \rangle &= \frac{N}{2M} \sum_{\bar{q}, l} \epsilon_l^\alpha(\bar{q}) v_{\bar{q}}^\alpha v_{-\bar{q}}^\beta \epsilon_l^\beta(\bar{q}) \\ &+ \frac{1}{2} \sum_{\bar{q}, l} \hbar\omega_l(\bar{q}) [n_l(\bar{q}) + \frac{1}{2}]. \end{aligned} \quad (6)$$

The $\langle \hat{\Phi} \rangle$ is calculated by taking the cumulant expansion for $\langle \exp[iq^\alpha(\hat{u}_i^\alpha - \hat{u}_j^\alpha)] \rangle$ to second order. The result is

$$\langle \hat{\Phi} \rangle = \frac{1}{2} \sum_{ij} \gamma_{ij} \sum_{q_1} V_{q_1} \exp[iq_1^\gamma (R_i^\gamma - R_j^\gamma)] \exp(-\frac{1}{2} q_1^\gamma q_1^\gamma \Gamma \gamma^\delta) \exp(iq_1^\gamma \langle u_i^\gamma - u_j^\gamma \rangle), \quad (7)$$

where $\Gamma \gamma^\delta$ is given by

$$\Gamma \gamma^\delta = 2(\langle \delta \hat{u}_i^\gamma \delta \hat{u}_i^\delta \rangle - \langle \delta \hat{u}_i^\gamma \delta \hat{u}_j^\delta \rangle) = \frac{1}{N} \sum_{q, l} \epsilon_l^\gamma(\bar{q}) \epsilon_l^\delta(\bar{q}) \frac{\hbar}{M\omega_l(\bar{q})} [2n_l(\bar{q}) + 1] \{1 - \exp[iq^\alpha(R_i^\alpha - R_j^\alpha)]\}. \quad (8)$$

The calculation of $\langle \hat{U} \rangle$ is carried out in the same fashion resulting in the equations

$$\langle \hat{U} \rangle = \sum_j \sum_{\bar{G}} U_{\bar{G}} \exp(iG^\gamma R_j^\gamma) \exp(iG^\gamma \langle u_j^\gamma \rangle) \exp(-G^\alpha G^\beta W^{\alpha\beta}), \quad (9)$$

where

$$W^{\alpha\beta} = \frac{1}{2} \langle \delta u_i^\alpha \delta u_j^\beta \rangle = \frac{1}{2N} \sum_{q, l} \epsilon_l^\alpha(\bar{q}) \epsilon_l^\beta(\bar{q}) \frac{\hbar}{M\omega_l(\bar{q})} [n_l(\bar{q}) + \frac{1}{2}]. \quad (10)$$

Minimization of F with respect to $n_l(\bar{q})$ gives

$$n_l(\bar{q}) = \{ \exp[\beta \hbar \tilde{\omega}_l(\bar{q})] - 1 \}^{-1}, \quad (11)$$

where $\beta = (k_B T)^{-1}$ and $\tilde{\omega}_l(\bar{q})$ is defined by

$$\hbar \tilde{\omega}_l(\bar{q}) = \frac{\delta \langle H \rangle}{\delta n_l(\bar{q})}. \quad (12)$$

Carrying out the indicated variations we find

$$\hbar \tilde{\omega}_l(\bar{q}) = \frac{1}{2} \hbar \omega_l(\bar{q}) + \frac{1}{2} \frac{\hbar}{\omega_l(\bar{q})} \epsilon_l^\alpha(\bar{q}) D^{\alpha\beta}(\bar{q}) \epsilon_l^\beta(\bar{q}). \quad (13)$$

We have defined the dynamical matrix $D^{\alpha\beta}(\bar{q}) = D_1^{\alpha\beta} + D_2^{\alpha\beta}(\bar{q})$;

$$D_1^{\alpha\beta} = \frac{1}{N} \sum_j \frac{1}{M} \sum_{\bar{G}} -G^\alpha G^\beta U_{\bar{G}} \exp(-G^\gamma G^\delta W^{\gamma\delta}) \exp(iG^\gamma \langle u_j^\gamma \rangle) \exp(iG^\gamma R_j^\gamma) \quad (14)$$

and

$$\begin{aligned} D_2^{\alpha\beta}(\bar{q}) &= \frac{1}{NM} \sum_{ij} \gamma_{ij} \sum_{q_1} -q_1^\alpha q_1^\beta v_{q_1} \exp[iq_1^\gamma (R_i^\gamma - R_j^\gamma)] \exp(iq_1^\gamma \langle u_i^\gamma - u_j^\gamma \rangle) \exp(-\frac{1}{2} q_1^\gamma q_1^\delta \Gamma \gamma^\delta) \\ &\times \{1 - \exp[iq_1^\gamma (R_i^\gamma - R_j^\gamma)]\}. \end{aligned} \quad (15)$$

Next the variation with respect to $v_{\vec{q}}^{\alpha}$ is carried out. It is immediately seen that $v_{\vec{q}}^{\alpha} = 0$ minimizes F , which means $\zeta_{\vec{q}, l}^* = \zeta_{-\vec{q}, l}$. The variation of F with respect to $\omega_l(\vec{q})$ gives

$$\omega_l^2(\vec{q}) = \epsilon_l^{\alpha}(\vec{q}) D^{\alpha\beta} \epsilon_l^{\beta}(\vec{q}) \quad (16)$$

and the minimization of F with respect to a set of orthonormal $\epsilon_l^{\alpha}(\vec{q})$ gives

$$D^{\alpha\beta}(\vec{q}) \epsilon_l^{\beta}(\vec{q}) = \omega_l^2(\vec{q}) \epsilon_l^{\alpha}(\vec{q}) \quad (17)$$

Comparison of Eq. (13) with Eq. (17) shows $\tilde{\omega}_l(\vec{q}) = \omega_l(\vec{q})$.

At this point if $u_{\vec{q}}^{\alpha}$ were set to zero, we would recover the standard SCP equations. The equations for the actual values are obtained by varying F with respect to $u_{\vec{q}}^{\alpha}$. The entropy and kinetic energy are independent of $u_{\vec{q}}^{\alpha}$, so we need only vary the potential-energy terms with respect to the parameter. We have after some manipulation

$$\frac{\delta \langle \hat{\Phi} \rangle}{\delta u_{\vec{q}}^{\alpha}} = \frac{i}{2} \sum_{ij} \gamma_{ij} \sum_{\vec{q}_1} V_{q_1} q_1^{\alpha} \exp[iq_1^{\gamma} (R_i^{\gamma} - R_j^{\gamma})] \exp(iq_1^{\gamma} \langle u_i^{\gamma} - u_j^{\gamma} \rangle) \exp(-\frac{1}{2} q_1^{\gamma} q_1^{\delta} \Gamma_{ij}^{\gamma\delta}) [\exp(iq^{\gamma} R_i^{\gamma}) - \exp(iq^{\gamma} R_j^{\gamma})] \quad (18)$$

and

$$\frac{\delta \langle \hat{U} \rangle}{\delta u_{\vec{q}}^{\alpha}} = i \sum_j \sum_G G^{\alpha} U_G \exp(iG^{\gamma} R_j^{\gamma}) \exp(iG^{\gamma} \langle u_j^{\gamma} \rangle) \exp(-G^{\gamma} G^{\delta} W^{\gamma\delta}) \exp(iq^{\gamma} R_j^{\gamma}) \quad (19)$$

These last two equations are quite complex and some approximation scheme is necessary in obtaining a solution. In Sec. III we examine these equations in the case that the $u_{\vec{q}}^{\alpha}$ are small, that is we examine the small distortion limit of the exact equations. This limit is valid for argon on graphite over a reasonable range of lattice constants.

III. LINEAR RESPONSE APPROXIMATION

The general equations for the strain amplitudes are significantly simplified when the strains are small. This condition is satisfied by rare-gas monolayers adsorbed on graphite except for those cases where the lattice constant is very close to the commensurate value of 4.26 Å. We assume that $\langle \hat{u}_j^{\alpha} \rangle \ll a$, where a is the lattice constant of the undistorted solid and expand the $\exp(iG \langle u_j^{\alpha} \rangle)$ term in a power series. Starting with Eq. (18), we ignore all terms which are higher order than linear in the $\langle \hat{u}_j^{\alpha} \rangle$. The term which is independent of $\langle \hat{u}_j^{\alpha} \rangle$ can be shown to be zero so only the linear term is needed. If we first define $D_{\delta^{\alpha\beta}}(\vec{q})$ to be the dynamical matrix in the absence of the strains with

$$D_{\delta^{\alpha\beta}}(\vec{q}) = \frac{1}{NM} \sum_{ij} \gamma_{ij} \sum_{\vec{q}_1} (-q_1^{\alpha} q_1^{\beta} V_{q_1}) \exp[iq_1^{\gamma} (R_i^{\gamma} - R_j^{\gamma})] \exp[-\frac{1}{2} q_1^{\gamma} q_1^{\delta} \Gamma_{ij}^{\gamma\delta}] [1 - \cos[\vec{q} \cdot (\vec{R}_i - \vec{R}_j)]] \quad (20)$$

Then we find that to first order in the $u_{\vec{q}}^{\alpha}$,

$$\frac{\delta \langle \hat{\Phi} \rangle}{\delta u_{\vec{q}}^{\alpha}} = NMD_{\delta^{\alpha\beta}}(\vec{q}) u_{-\vec{q}}^{\beta} \quad (21)$$

This term is linear in the $U_{\vec{G}}$ for small $u_{\vec{q}}^{\beta}$. If $w_l(\vec{q})$ and $e_l^{\alpha}(\vec{q})$ are the frequencies and polarization vectors determined by the diagonalization of $D_{\delta^{\alpha\beta}}(\vec{q})$ then

$$\frac{\delta \langle \hat{\Phi} \rangle}{\delta u_{\vec{q}}^{\alpha}} = MN \sum_l e_l^{\alpha}(\vec{q}) w_l^2(\vec{q}) e_l^{\beta}(\vec{q}) u_{-\vec{q}}^{\beta} \quad (22)$$

In Eq. (19), the term which is independent of $u_{\vec{q}}^{\alpha}$ is not zero, and so we retain only this term. Thus we have to first order in the $U_{\vec{G}}$

$$\frac{\delta \langle \hat{U} \rangle}{\delta u_{\vec{q}}^{\alpha}} = iN \sum_{\vec{G}} \sum_{\vec{\tau}} G^{\alpha} U_{\vec{G}} e^{-G^{\gamma} G^{\delta} W^{\gamma\delta}} \delta_{\vec{\tau}, \vec{G} + \vec{q}} \quad (23)$$

Setting the sum of $\delta \langle \hat{\Phi} \rangle / \delta u_{\vec{q}}^{\alpha}$ and $\delta \langle \hat{U} \rangle / \delta u_{\vec{q}}^{\alpha}$ equal to zero we find after some manipulation

$$\langle u_j^{\alpha} \rangle = \sum_{\vec{G}} \tilde{u}_{\vec{G}}^{\alpha} \sin[\vec{G} \cdot (\vec{R}_j - \vec{\Delta})] \quad (24)$$

where

$$\tilde{u}_{\vec{G}}^{\alpha} = \sum_{\Gamma} \frac{e_i^{\alpha}(\vec{G}) \tilde{U}_{\vec{G}} e^{-G\gamma G^{\delta} W\gamma^{\delta}}}{Mw^2(\vec{G})} e^{\beta}(\vec{G}) G^{\beta} \quad (25)$$

Equations (24) and (25) have been written in the periodic Brillouin-zone scheme. The quantities $\tilde{u}_{\vec{G}}^{\alpha}$ and $\tilde{U}_{\vec{G}}$ are the "moduli" of the complex quantities $u_{\vec{G}}^{\alpha}$ and $U_{\vec{G}}$ with

$$u_{\vec{G}}^{\alpha} = -i\tilde{u}_{\vec{G}}^{\alpha} \exp(-i\vec{G} \cdot \vec{\Delta})$$

and

$$U_{\vec{G}} = \tilde{U}_{\vec{G}} \exp(-i\vec{G} \cdot \vec{\Delta})$$

Both $\tilde{u}_{\vec{G}}^{\alpha}$ and $\tilde{U}_{\vec{G}}$ are real with $\tilde{u}_{\vec{G}}^{\alpha}$ being antisymmetric in \vec{G} and $\tilde{U}_{\vec{G}}$ being symmetric. The "phase" $\vec{\Delta}$ is the displacement between a center of symmetry of the substrate and the origin (which is a center of symmetry of the undistorted lattice).⁹ Equations (24) and (25) are essentially those of Novaco and McTague with the exception that both adatom-adatom and adatom-substrate coupling constants are now renormalized by the motion of the adatom. For the adatom-substrate coupling, this renormalization appears through the

$$\exp(-\frac{1}{2} G\gamma G^{\delta} \langle \delta \hat{u}_i^{\gamma} \delta \hat{u}_i^{\delta} \rangle)$$

term in Eq. (25).

The evaluation of the $\langle \hat{H} \rangle$ is relatively straightforward in the small distortion limit. Expanding the $\exp(iq_1^{\gamma} \langle \hat{u}_i^{\gamma} \rangle)$ term in Eq. (7) as a power series in the $u_{\vec{q}}^{\alpha}$ and retaining the first three terms gives the energy to second order in the $U_{\vec{G}}$. Since the linear term is zero due to symmetry we find

$$\begin{aligned} \langle \hat{\phi} \rangle &= \frac{1}{2} \sum_{ij} \gamma_{ij} \sum_{q_1} V_{q_1} \exp[iq_1^{\gamma} (R_i^{\gamma} - R_j^{\gamma})] \\ &\quad \times \exp(-\frac{1}{2} q_1^{\gamma} q_1^{\delta} \Gamma_{ij}^{\gamma\delta}) \quad (26) \\ &\quad + \frac{1}{2} NM \sum_{\vec{q}} u_{\vec{q}}^{\alpha} D_{\vec{q}}^{\alpha\beta} u_{-\vec{q}}^{\beta} \end{aligned}$$

Following the same procedure for the $\langle \hat{U} \rangle$, but retaining only the first two terms in the expansion of the exponential we find to second order in $U_{\vec{G}}$ that

$$\begin{aligned} \langle \hat{U} \rangle &= N \sum_{\vec{G}} \Delta(\vec{\tau}) U_{\vec{G}} \exp(-G\gamma G^{\delta} W\gamma^{\delta}) \\ &\quad + iN \sum_{\vec{G}} U_{\vec{G}} \exp(-G\gamma G^{\delta} W\gamma^{\delta}) G^{\gamma} u_{-\vec{G}}^{\gamma} \quad (27) \end{aligned}$$

The energy term of the right-hand side of Eq. (26) which is independent of $U_{\vec{G}}$ is just the usual potential-energy term associated with the motion of the atom. The second term is positive energy contri-

bution associated with the strains in the monolayer generated by the MDWs. The first term on the right in Eq. (27) is an energy gain associated with the undistorted solid and it is nonzero only for commensurate structures. The second term is the energy gain associated with the MDWs. Both terms associated with the MDWs can be combined to give

$$E_{\text{MDW}} = -\frac{1}{2} N \sum_{\vec{G}} \tilde{U}_{\vec{G}} \exp(-G\gamma G^{\delta} W\gamma^{\delta}) G^{\beta} \tilde{u}_{\vec{G}}^{\beta} \quad (28)$$

For the incommensurate structure this is the only energy term associated with the substrate field. This term is independent of $\vec{\Delta}$ showing that (in this approximation) the energy of the system is invariant to translations of the monolayer relative to the substrate.

The physics of the orientational epitaxy phase is the same here as in the original calculation of Novaco and McTague. We outline here the reasons for the alignment of the monolayer crystal axes away from those of the substrate and refer the reader to Ref. 9 for more complete details. The misorientation of the monolayer and substrate is caused by the competition between the $[w_l(\vec{q})]^{-2}$ and the $G^{\alpha} \epsilon^{\beta}(\vec{q})$ terms in Eq. (25). The MDW energy at fixed angle is, as can be seen from Eqs. (25) and (28), proportional to the product of the first term and the square of the second, this product then summed over the mode index l . Those orientations with large strains are associated with large energy shifts (although the two functions do not peak at *exactly* the same angle). The $[w_l^2(\vec{q})]^{-2}$ term favors small \vec{q} orientations thus tending to align the crystal axes. However, when the crystal axes are exactly aligned, the second term is identically zero for the transverse branch. Since the transverse branch is softer [smaller $w(\vec{q})$] it will be advantageous for the system to rotate away from the symmetry direction *if* the transverse branch is low enough. This is the case for the rare-gas on graphite systems except for those lattice constants very close to the registered state value. Only for krypton is this state important, the other systems tending to find equilibrium away from the registered state.

IV. LATTICE DYNAMICS AND ORIENTATIONAL EPITAXY OF ARGON

The argon monolayer on a graphite substrate has been studied experimentally by both neutron scattering¹⁷ and low-energy electron diffraction (LEED) techniques.¹¹ The neutron experiments have produced a wealth of information on the "average" structure of the monolayer and its lattice dynamics. The LEED study shows both the structure of the argon and its orientation relative to the graphite surface crystal axes. Both techniques had associated experimental difficulties which make the observation of struc-

ture factor satellite peaks difficult to observe. These satellites might be observable in an x-ray experiment.¹⁸ The quasiharmonic (QH) predictions of Novaco and McTague agree quite well with experimental results, but the SCP corrections to the lattice dynamics of this system are not negligible. Thus we choose this important and well characterized system as the one to study first within the SCP approximation.

The initial step in the SCP calculation is the generation, at various lattice constants, of solutions to the SCP equations in zero external field. This requires the iteration of Eqs. (8) and (20) along with the eigenvalue equation for $D_0^{\alpha\beta}(\vec{q})$. We assume that the argon-argon interaction on the graphite surface is well approximated by their interaction in vacuum so that we may choose one of the standard Lennard-Jones (12-6) interactions without serious error. The ϵ_0 and σ values, taken from Ref. 19, are listed in Table I. Since the Lennard-Jones interaction does not have a Fourier transform, Eq. (20) must be rewritten in real space and the real-space integration truncated at very small interatomic distances. This transformation from momentum space to real space

TABLE I. Parameters for the argon-argon and argon-graphite interactions. The argon-argon interaction is a Lennard-Jones (12-6) potential with minimum energy ϵ_0 and "hard-core" radius of σ . The argon-graphite interaction is represented by the six (equal) Fourier coefficients associated with the \vec{G} vectors generated by symmetry from $G_1 = 4\pi/(3)^{1/2}a$.

argon-argon	argon-graphite
$\sigma = 3.40 \text{ \AA}$	$U_{\vec{G}_1} = -4.7 \text{ K}$
$\epsilon_0 = 119 \text{ K}$	

is quite standard²⁰ and we only quote the final results. Defining the coupling constants $\overline{\Phi}_{ij}^{\alpha\beta}$ via the equation

$$D_0^{\alpha\beta}(\vec{a}) = \frac{1}{NM} \sum_{ij} \gamma_{ij} \overline{\Phi}_{ij}^{\alpha\beta} \{1 - \cos[\vec{q} \cdot (\vec{R}_i - \vec{R}_j)]\} , \quad (29)$$

we find

$$\overline{\Phi}_{ij}^{\alpha\beta} = \frac{1}{2\pi(\det \vec{F})^{1/2}} \int_{-\infty}^{\infty} du^x \int_{-\infty}^{\infty} du^y v^{\alpha\beta}(\vec{R}_j - \vec{R}_i + \vec{u}) \exp[-\frac{1}{2} \Gamma \gamma^{\delta} u^{\gamma} u^{\delta}] , \quad (30a)$$

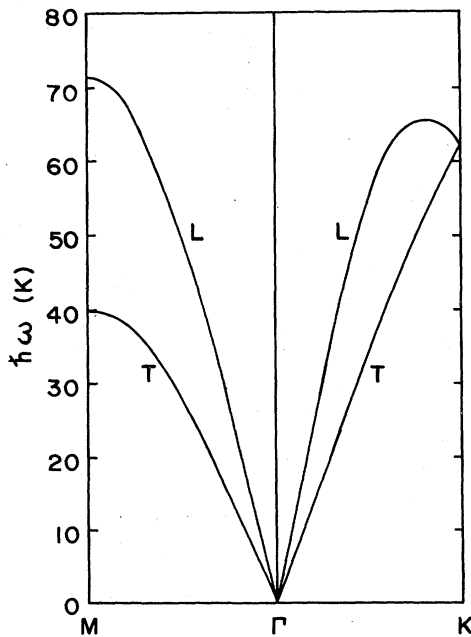


FIG. 1. The phonon spectrum along high-symmetry directions in the Brillouin zone. The notation of Ref. 17 is used. The calculation was done within the SCP approximation at a lattice parameter of 3.86 \AA .

with $v^{\alpha\beta}$ being the second derivative of the real-space potential $v(\vec{r})$ and given by

$$v_{\vec{r}}^{\alpha\beta} = \frac{\partial}{\partial r^{\alpha}} \frac{\partial}{\partial r^{\beta}} v(\vec{r}) . \quad (30b)$$

The matrix \vec{F}^{-1} is the inverse of \vec{F} defined by Eq. (8). The third-nearest-neighbor SCP spectrum for argon at a lattice constant of 3.86 \AA is shown in Fig. 1. The phonon frequencies in the SCP approximation are about 15% higher than in the corresponding QH calculation. This can be readily seen upon examining Table II which lists $\hbar\omega$ for zone-boundary phonons at $a = 3.82$ and 3.86 \AA in both the SCP and

TABLE II. Zone-boundary phonon frequencies for both SCP and QH calculations.

a (\AA)	$\hbar\omega_L(M)$ (meV)	$\hbar\omega_T(M)$ (meV)	$\hbar\omega_L(K) = \hbar\omega_T(K)$ (meV)
3.82	QH: 5.90	3.35	5.11
	SCP: 6.74	3.77	5.81
3.86	QH: 5.28	3.04	4.59
	SCP: 6.14	3.46	5.30

QH schemes. The neutron scattering experiments for $a = 3.86 \text{ \AA}$ agree quite well with a QH calculation using coupling constants calculated for the same Lennard-Jones interaction we use but with $a = 3.82 \text{ \AA}$.¹⁷ Note from Table II that although the SCP corrections are large, the SCP values for $\hbar\omega$ at 3.86 \AA are quite close to the QH values at 3.82 \AA . Given the constraints and uncertainties of the neutron scattering results, our SCP phonon frequencies at 3.86 \AA are quite consistent with the neutron data. Both the QH and SCP third-nearest-neighbor calculations predict 3.86 \AA to be the zero-pressure lattice parameter at zero temperature. This is in excellent agreement with the neutron studies.¹⁷ It would seem then that any effects on the argon-argon interaction due to the presence of the graphite substrate are small enough that we may neglect them for the purposes of this calculation. We might add that uncertainties in the Lennard-Jones parameters for the argon-argon interaction in vacuum also are small enough that we may neglect their effects. The values of $U_{\bar{c}}$ were taken from Steele's paper²¹ on the interaction of rare-gas atoms with graphite and are listed in Table I. Only the lowest six coefficients were used, these six are equal to each other because of the six fold symmetry of the graphite surface basal plane. The orientation of the argon is independent of $U_{\bar{c}}$ if

only these lowest terms are used.²² The orientation also appears to be relatively insensitive to the inclusion or exclusion of realistic estimates for higher $U_{\bar{c}}$ terms.

Once the phonon frequencies and polarization vectors have been calculated at some chosen value of a , the energy associated with the MDWs can be calculated as a function of rotation angle θ , the angle between the argon crystal axes and that of the graphite. We use the same angle as that in Ref. 9. This energy is shown in Fig. 2 at $a = 3.86 \text{ \AA}$ for both the QH and SCP calculations. Note that the SCP curve has much the same shape as the QH curve, but the magnitude of E_{MDW} is reduced by about 40%. The reduction in E_{MDW} reflects a corresponding decrease in $u_{\bar{c}}^{\alpha}$ and is due to both the increase in the phonon frequencies and the renormalization of the $U_{\bar{c}}$ due to the SCP corrections.

The energy of the system in the SCP approximation can now be calculated as a function of a . The $\langle \hat{\phi} \rangle$ is calculated by transforming the first term in Eq. (26) to real-space. The $\langle \hat{U} \rangle$ is given by Eq. (27). Figure 3 shows both E_0 (the zero-field energy) and $E_T = (E_0 + E_{MDW})$ as a function of a for both QH and SCP calculations. Note that the zero-pressure lattice

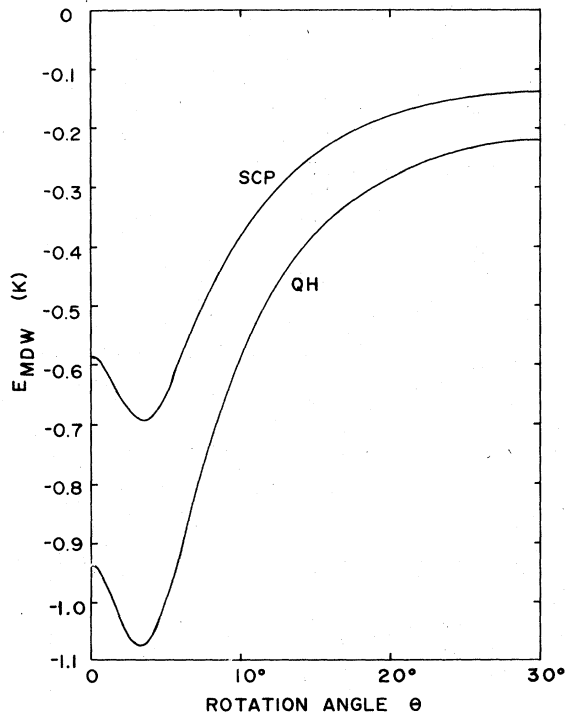


FIG. 2. The mass-density wave contribution to the energy plotted as a function of the angle θ . The curves show both the SCP calculation and the QH calculation at a lattice parameter of 3.86 \AA .

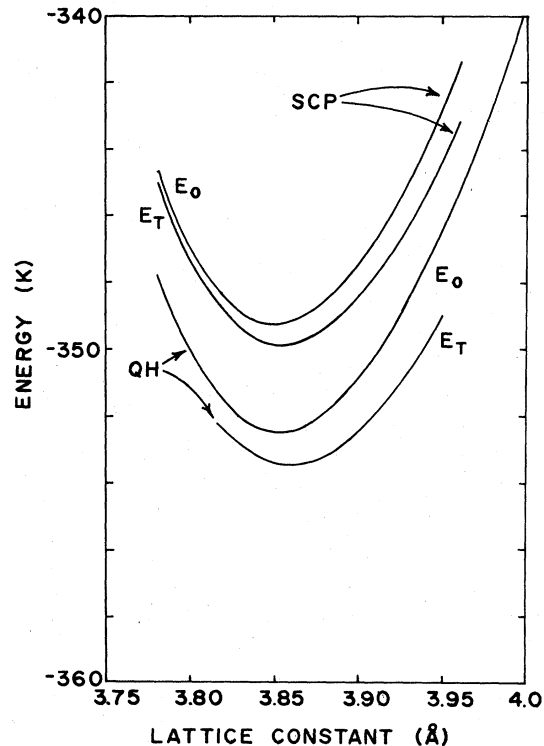


FIG. 3. The zero-strain energy E_0 and the total energy E_T plotted as a function of the lattice parameter. Both SCP and QH calculations are shown.

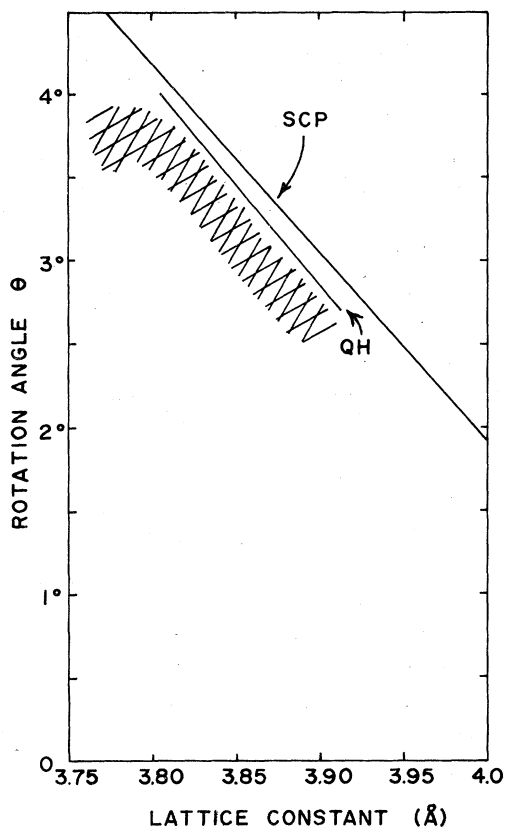


FIG. 4. The equilibrium orientation angle θ as a function of lattice parameter for both SCP and QH calculations. The shaded region indicates where the experimental values of Ref. 11 lie.

constant is about 3.86 \AA in both cases. This value is determined mostly by E_0 , E_{MDW} having only a very small effect. The zero-point energy contribution to E_0 is responsible for increase in A beyond its classical value of about 3.82 \AA .

Figure 4 shows the rotation angle θ as a function of lattice parameter for both QH and SCP calculations. Note that the SCP correction to this curve is very small. The experimental points lie in the shaded region. The general agreement is very good except at the higher angles. Here, the shift of the data away from the theoretical curve appears to be a result of extrinsic experimental effects.¹¹ Nevertheless, there is a systematic difference between theory and experiment.

V. DISCUSSION

The SCP corrections to the phonon frequencies of the argon monolayer at 0 K are important and are large enough to be observable in an inelastic-neutron-scattering experiment. The neutron study of

adsorbed argon was sensitive to the large density of states near the zone-boundary modes. The QH calculation at 3.86 \AA gives zone-boundary modes which are definitely too low, while the SCP results at 3.86 \AA are in good agreement with the data. Note that the 15 to 20% increase in the mode frequencies alters the rotation angle by only 0.2° . This angle is largely determined by the ratio of transverse to longitudinal²² sound velocities and this ratio is only slightly affected by the SCP corrections. Although finite temperature effects would alter the mode frequencies, they are unlikely to alter the sound velocity by any significant factor until the system is very close to the melting transition. Thus it is reasonable to expect the zero-temperature SCP results to be a good estimate of the experimental results outside the melting region. The LEED data was taken at temperatures between 30 and 50 K while the melting of the argon layer begins at about 50 K.¹⁷

It is worthwhile, at this point, to discuss the relevance of the Mermin theorem to the above equations when applied to two-dimensional systems at finite temperatures. It is well known that many physically important quantities are well defined even in the presence of the long-wavelength divergences associated with this theorem.²³ This is certainly true for the correlation function $\langle \delta \hat{u}_i^\alpha \delta \hat{u}_i^\beta - \delta \hat{u}_i^\alpha \delta \hat{u}_j^\beta \rangle$ which is used in calculating the phonon frequencies. However, the same is not true of the $\langle \delta \hat{u}_j^\alpha \delta \hat{u}_j^\beta \rangle$ term used to calculate $\langle \hat{u}_j^\alpha \rangle$ since this formally diverges. This formal divergence is, however, not a strong one (it goes as $\ln N$) and there are a number of considerations which will result in a finite value of $\langle \delta \hat{u}_j^\alpha \delta \hat{u}_j^\beta \rangle$. The finite size of the real system will certainly provide a natural long-wavelength cutoff for the phonon modes resulting in a finite value of the average-square displacement. There is also the fact that the monolayer is adsorbed on a substrate with its own dynamics, and the very long-wavelength phonons of the monolayer are just the ones which are strongly coupled to the substrate phonon modes.²⁴ Furthermore the orientational epitaxy phase will have (exact) transverse "phonons" with a gap at zero \bar{q} due to the removal of the rotational symmetry from the problem. If the substrate is now allowed to deform, it is reasonable to believe that the only mode with zero frequency will be that mode which corresponds to the rigid movement of both the substrate and the monolayer. The long-wavelength modes which correspond to the relative moment of each in the direction parallel to the surface should have a gap. It is this relative movement which defines the renormalized coupling constant to the surface. All of the above aspects of the problem must be considered in a full treatment of the finite temperature properties of the orientational epitaxy phase in real systems, especially near an incommensurate-commensurate phase transition.

Finally, a few remarks are in order about the terms

which are ignored in the small distortion limit. These missing terms show that the $U_{\vec{q}}$ generate $\{u_{\vec{q}_1}^{\alpha}\}$ which then generate $\{u_{\vec{q}_2}^{\beta}\}$, etc. The \vec{q}_2 terms are higher harmonics, thus demonstrating that as the distortions increase in amplitude, they are no longer pure sine waves. Similar effects can be seen in a more general treatment of the dynamical matrix. In this case one finds that the MDWs couple phonon modes of different \vec{q} vectors so that the true excitations of the system are linear combinations of phonon modes. This combination of mode mixing and generation of higher harmonics must be an important part of any phase transitions between commensurate and incommensurate states. One would expect these higher harmonics to place as many atoms on absorption sites as possible, this taking place at the expense of a few atoms which will be far from registry and separate the regions where the atoms do nearly register. Thus, as the commensurate phase is approached from the incommensurate phase, there appear domains in the monolayer system with boundaries

that are, at first, very diffuse and ill defined. As the system gets closer and closer to the phase transition, these domains grow in size and become better defined with sharper domain boundaries. This phenomenon is related to dislocation networks in adsorbed layers and to solitons in one-dimensional conductors.^{2, 25-28} The problem of orientational epitaxy and the incommensurate to commensurate phase transition will continue to provide an exciting area of research for the future.

ACKNOWLEDGMENTS

I wish to thank Dr. J. P. McTague and Dr. V. J. Emery for helpful discussions on a number of aspects of this problem. At Lafayette College, Penn., research was supported in part by NSF under Grant No. DMR 75-15630. Research at Brookhaven supported in part by the Division of Basic Energy Sciences, DOE, under Contract No. ET-76-C-02-0016.

¹See, for example, *Epitaxial Growth*, edited by J. W.

Matthews (Academic, New York, 1975), Part B, Chaps. VI-VIII.

²F. C. Frank and J. H. van der Merwe, Proc. R. Soc. London, Ser. A **198**, 205, 216 (1949); **200**, 125 (1949).

³J. A. Snyman and J. H. van der Merwe, Surf. Sci. **42**, 190 (1974); **45**, 619 (1974).

⁴S. C. Ying, Phys. Rev. B **3**, 4160 (1971).

⁵J. G. Dash, *Films on Solid Surfaces* (Academic, New York, 1975).

⁶W. A. Steele, *The Interaction of Gases with Solid Surfaces* (Pergamon, Oxford, 1974).

⁷J. D. Axe, in *Proceedings of the Conference on Neutron Scattering, Gatlinburg, Tennessee, 1975*, edited by R. M. Moon (National Technical Information Service, Springfield, Virginia, 1976), p. 353.

⁸V. J. Emery, in *Chemistry and Physics of One-Dimensional Metals*, edited by H. J. Keller (Plenum, New York, 1977).

⁹A. D. Novaco and J. P. McTague, Phys. Rev. Lett. **38**, 1286 (1977); J. Phys. (Paris) **38**, C4-116 (1977).

¹⁰M. D. Chinn and S. C. Fain, Jr., Phys. Rev. Lett. **39**, 146 (1977).

¹¹C. G. Shaw, S. C. Fain, Jr., and M. D. Chinn, Phys. Rev. Lett. **41**, 955 (1978).

¹²N. D. Werthamer, in *Rare Gas Solid*, edited by M. L. Klein and J. A. Venables (Academic, New York, 1976).

¹³N. D. Mermin, Phys. Rev. **176**, 250 (1968).

¹⁴The usual treatment involves a variational calculation in

real space (see Ref. 12). For the current problem it is more convenient to carry out the variational calculation in momentum space, but the results for zero external field are identical to the results of the real-space calculation.

¹⁵See, for example: K. Huang, *Statistical Mechanics* (Wiley, New York, 1963), p. 196.

¹⁶See, for example: C. Kittel, *Quantum Theory of Solids* (Wiley, New York, 1963), p. 395.

¹⁷H. Taub, K. Carneiro, J. K. Kjems, L. Passell, and J. P. McTague, Phys. Rev. B **16**, 4551 (1977).

¹⁸D. Moncton (private communication).

¹⁹G. K. Horton, in *Rare Gas Solids*, edited by M. L. Klein and J. A. Venables (Academic, New York, 1976), Vol. I.

²⁰M. L. Klein and T. R. Koehler, in *Rare Gas Solids*, edited by M. L. Klein and J. A. Venables (Academic, New York, 1976), Vol. I.

²¹W. A. Steele, Surf. Sci. **36**, 317 (1973).

²²A. D. Novaco and J. P. McTague (unpublished).

²³Y. Imry and L. Gunther, Phys. Rev. B **3**, 3939 (1971) and references cited therein.

²⁴J. P. McTague and A. D. Novaco, Phys. Rev. B **19**, 5299 (1979).

²⁵J. A. Venables and P. S. Schabes-Retchkiman, J. Phys. (Paris) **38**, C4-105 (1977).

²⁶P. Bak and V. J. Emery, Phys. Rev. Lett. **36**, 978 (1976).

²⁷W. L. McMillan, Phys. Rev. B **14**, 1496 (1976).

²⁸J. Villian, Phys. Rev. Lett. **41**, 36 (1978).